

Garber Laboratories, Inc.

Corrosion Engineering, Consulting, and Testing Services

P.O. Box 51641 Lafayette, LA 70505 Office: 337-237-2342 Fax: 337-237-8982

December 22, 2011

Mr. John Trosclair
Block T Petroleum
P.O. Box 2080
Tyler, TX 75710-2080

Re: Project Number 11-417, Failure Analysis of a 2 7/8-Inch L-80 Production Tubing
Location: South Bayou Malett Field, Thibodeaux Lease, Well # 1

INTRODUCTION:

The 2 7/8-inch production tubing from the Thibodeaux #1 well has suffered several corrosion related failures after 3 years and 8 months of service. After flowing for 8 months, the well was converted to a pumping well on December 8, 2008. After 7 months of pumping, the well was converted to a gas lift well on July 15, 2009. The tubing was inspected and because there was no indication of corrosion, none of the joints were replaced. The well had been on gas lift for 28 months when the failures were reported. The recent production rates were 20 bbls/day of oil, 1,000 bbls/day of water, and 165 mscf/day of gas, which included the lift gas. The gas contained approximately 1.0 % CO₂ and some H₂S. The produced water had a chloride content of 44,200 mg/l and a relatively high acetate concentration of 1,200 mg/l. The flowing wellhead conditions were 240 psig and 115 °F. The bottom hole pressure was reported to be 3,723 psig. Figure 1 shows the nine sections of the tubing that were received for examination. The sections came from various depths ranging from 500 feet to 8,700 feet. Figure 2 shows the two gas lift mandrels that were also received for examination. They were reported to be the bottom gas lift mandrels, which were located at 3,860 feet and 4,155 feet. The total tubing depth was approximately 8,893 feet.

It was the objective of this investigation to determine the most likely mechanism of the failures, and to recommend ways of preventing them from happening again. The test procedures conducted on the 2 7/8-inch tubing and gas lift mandrels included:

1. Visual examination
2. Several sections were cut open
3. Photographs of the metal surfaces
4. Analyses of internal and external scales
5. Physical measurements and calculated corrosion rates

6. Hardness measurements
7. Fluid velocity calculations

CONCLUSIONS:

1. Several corrosion mechanisms were identified. These included rod wear that cold worked the tubing, removed protective scales, and accelerated the corrosion process, CO₂ pitting corrosion that was assisted by H₂S, and flow-induced sand impingement at the leading edge of the pin ends. These three corrosion mechanisms had originated from the internal surface. In addition to the internal corrosion, the two gas lift mandrels and one of the tubing sections had suffered external corrosion that appeared to be caused by bacteria.
2. The most aggressive corrosion mechanism appeared to be the external bacterial corrosion. Since the tubing had been inspected in May of 2010 with no indication of corrosion, these failures occurred in less than 18 months. Based on the nominal wall thickness, the calculated average corrosion rate at the failure sites was approximately 150 mils/year (mpy).
3. All of the failure sites that originated from the internal surface were associated with rod wear. It appeared that the rubbing of the rods against the tubing had removed protective scale and had cold worked the metal surface, which allowed aggressive corrosion attack to occur. The mesa morphology of the pits and the abundance of siderite in the pits were consistent with CO₂ corrosion.
4. It appeared that most of the CO₂ corrosion occurred after the well was converted to gas lift since most of the pits exhibited a flow-induced component. The presence of iron sulfide in the pits suggested that H₂S had contributed to the corrosion process.
5. Several sections had failure sites on opposite sides of the tubing. The initial penetration was in the rod wear area. Once the tubing was penetrated, the flow of gas and fluids from the annulus into the tubing created an area of impingement opposite the initial failure site, which resulted in the second failure site.
6. The pin end from 2,900 feet had suffered severe sand impingement at the leading edge of the pin. The pin end from 3,300 feet exhibited minor sand impingement. The flow dynamics calculations indicated that the sand impingement occurred after the well was converted to gas lift. The flow dynamics in the tubing before the well was converted to gas lift would not have generated the velocities needed to produce this level of metal loss.
7. The pin end from 3,300 feet had also suffered external corrosion. The corrosion was one large deep pit. The morphology of this pit and the abundance of iron sulfide in the pit indicated that the corrosion was due to bacteria.

8. The two gas lift mandrels had suffered external corrosion. Again, the morphology of these pits and the abundance of iron sulfide in the scale were consistent with bacterial corrosion.
9. The analysis of the scale from the internal surface identified magnetite, which was believed to be mill scale from the manufacturing process, sand, which would have contributed to impingement and erosion, siderite, which was the product of CO₂ corrosion, calcite, which was a mineral scale, and iron sulfide, which was the product of H₂S corrosion. The abundance of siderite indicated that CO₂ was the primary corrosive specie. The presence of iron sulfide indicated that H₂S had contributed to the corrosion process.
10. The analysis of the scale from the external surface identified sand, iron sulfide, and siderite. The abundance of iron sulfide indicated that H₂S was the primary corrosive specie. The morphology of the pits suggested that the source of the H₂S was sulfate-reducing bacteria (SRB).
11. The water analysis indicated a very large concentration of acetates, 1,200 mg/l, which could have contributed to the CO₂ corrosion process.
12. The physical measurements verified that the tubing was 2 7/8-inch, 6.5 #/ft material. The hardness measurements indicated that the tubing was L-80 grade as reported.
13. The flow dynamics calculations indicated that the flow in the tubing during the initial flowing and pumping conditions would not have generated enough velocity or turbulence to produce sand impingement or a flow-induced environment because the fluid velocities were less than 0.8 ft/sec. However, the fluid velocities after the well was converted to gas lift increased to 15.9 ft/sec, which would have promoted sand impingement and flow-induced CO₂ corrosion.

RECOMMENDATIONS:

1. If any of the original tubing is currently in the well, the tubing should be removed and inspected for internal and external corrosion. Any joint of tubing that has experienced cold working due to rod wear from the sucker rods should be discarded. It might be best to eliminate all of the original tubing.
2. Since this well is now on gas lift, the problem with future rod wear will no longer exist. However, the well fluids exhibited a corrosive nature and plans should be made to introduce a corrosion inhibitor into the well to control internal CO₂ and H₂S corrosion.
3. The problem with sand impingement has to be addressed. Eliminating the sand with sand screens or gravel packs should end this problem. If the sand cannot be eliminated, tubing collars that eliminate the gap in between the joints should be used. Either premium connectors or collars with inserts could eliminate the exposure of the leading edge of the pin.

4. The bacteria infestation in the annulus will have to be addressed. Bactericide applications should resolve this problem. Since the external corrosion due to bacteria was so aggressive, there is the possibility of corrosion damage to the internal surface of the casing. A caliper survey should be conducted on the casing to determine the integrity of the casing.
5. Replacing the L-80 tubing with corrosion resistant alloy (CRA), like chrome 13, should solve the internal corrosion problems, but the problem with sand impingement and bacteria will remain and will have to be addressed.

EXPERIMENTAL RESULTS:

Experimental tests were performed on the failed tubing and gas lift mandrels to assist in determining the most likely cause of the failures. A summary of these results follows:

1. Visual examination

A total of nine sections of the tubing and two gas lift mandrels were received for examination. Figure 1 shows the nine sections of the tubing and Figure 2 shows the two gas lift mandrels. The tubing sections were from various depths in the well ranging from 500 feet to 8,700 feet. Six of these sections were carefully examined in an attempt to determine the mechanism of the failures. These sections were from depths of 1,800, 2,900, 3,300, 5,700, 6,800 and 8,700 feet.

Section #2; 1,800 feet: Figure 3 shows the external surface of the section from 1,800 feet. There was a large failure site. Other than the failure site there was no evidence of external corrosion. The section was split open to facilitate an examination of the internal surface. Figure 4 shows the internal surface of the tubing. The failure was located in a trench that appeared to be from rod wear. There was also a large circular area of metal loss that was on the opposite side of the tubing from the failure site. It appeared that this metal loss was due to liquid/sand impingement that occurred after the tubing wall was penetrated. The metal surface was coated with a thin layer of dark brown scale. The scale was removed and samples were collected for further analysis. Figure 5 shows the internal surface after cleaning. There was a significant amount of corrosion around the failure site, which indicated that the corrosion had initiated from the internal surface. Figure 6 shows a closer view of the failure site. There was a line of very deep pits that appeared to be in an area where the sucker rod rubbed against the side of the tubing.

Section #3; 2,900 feet: Figure 7 shows the pin end of this section. The threads had suffered significant metal loss. The metal loss appeared to be due to impingement on the threads that were facing the direction of flow. Figure 8 shows a closer view of the threads. The amount of metal loss was significant. Other than the impingement, there was no significant internal or external corrosion on this section.

Section #4; 3,300 feet: Figure 9 shows the pin end from this section. This section had one very large and deep pit on the external surface near the threads. The pit was cleaned and Figure 10

shows a closer view of the pit after cleaning. The morphology of the pit with smooth surfaces, slightly undercut edges, tiered sides, and a broad flat bottom suggested that bacteria were responsible for the corrosion. The leading edge of the threads had suffered a slight amount of impingement, but no additional internal or external corrosion was noted.

Section #6; 5,700 feet: Figure 11 shows the external surface of this section. There was a line of failure sites on the external, but no other external corrosion was noted. The section was split open to facilitate an examination of the internal surface. Figure 12 shows the internal surface of this section. There was a line of corrosion pits on one side, but no other internal corrosion was noted. The surface was coated with a thin layer of tenacious gray scale. The scale was removed and samples were collected for further analysis. Figure 13 shows the internal surface after cleaning. All of the corrosion damage was isolated to a trench that appeared to have been damaged by the sucker rod. Figure 14 shows a closer view of the corrosion. It was obvious that the corrosion had initiated from the internal surface. Most of these pits exhibited the mesa morphology that is associated with CO₂ corrosion. Some of the pits exhibited an elongated shape that is associated with a flow-induced component. There were also areas of shiny metal that appeared to be caused by the rod rubbing against the side of the tubing.

Section #7; 6,800 feet: Figure 15 shows the external surface of this section. This section had two failure sites on opposite sides of the tubing. In addition to the failure sites, there was some moderate external mesa corrosion adjacent to the large hole. The section was split open and the thin layer of gray scale that was on the internal surface was removed. Figure 16 shows the internal surface after cleaning. Again, the bulk of the corrosion damage was isolated to a trench that appeared to be the result of the rod rubbing against the tubing. The second failure site was directly opposite the larger hole and appeared to be the result of fluid impingement after the first failure occurred.

Section #9; 8,700 feet: Figure 17 shows the external surface of this section. There was a line of failure sites, but no other evidence of external corrosion. The section was split open and the surface scales were removed. Figure 18 shows the internal surface after cleaning. Again, there was evidence of rod wear and all of the internal corrosion was isolated to the trench that was created by the rod.

Gas lift mandrel from 3,860 feet: Figure 19 shows two very large failure sites that were present on this mandrel. The corrosion appeared to be external in origin. An inspection of the internal surface did not reveal any significant corrosion. The area around the failure sites was cleaned and samples of the surface scales were collected for further analysis. Figure 20 shows a closer view of the failure sites after cleaning. This morphology with smooth surfaces, tiered sides, slightly undercut edges, and broad flat bottoms was consistent with bacterial corrosion.

Gas lift mandrel from 4,100 feet: Figure 21 shows two deep pits that were present on the external surface of the mandrel. The failure site is shown in Figure 22. This area was cleaned and samples of the scale were collected for further analysis. Figure 23 shows a closer view of the failure site after cleaning. It appeared that this corrosion had initiated from the external surface and although there was an extensive amount of metal loss, the morphology of the pits resembled

bacterial corrosion. Figure 24 shows some mechanical damage that was present on the mandrel adjacent to the failure site. It was not determined if this damage had contributed to the failure.

2. Scale analysis

The scales that were collected from the internal and external surfaces were analyzed using wet bench methods. The following results were obtained:

<u>Compound</u>	<u>Weight % Internal</u>	<u>Weight % External</u>
Magnetite (Fe ₃ O ₄)	36 %	6 %
Acid Insoluble material	19 %	57 %
Siderite (FeCO ₃)	18 %	12 %
Calcite (CaCO ₃)	12 %	Negative
Iron Sulfide (FeS)	11 %	20 %
Hematite (Fe ₂ O ₃)	4 %	5 %

The magnetite was believed to be a result of the fabrication process. The acid insoluble material appeared to be sand. The major corrosion products were siderite from CO₂ corrosion and iron sulfide from H₂S corrosion. The scale from the internal surface also contained some calcite (calcium carbonate), which deposited from the produced water. The scale from the external surface contained a significant amount of organic material, which was believed to be biomass from bacterial activity. The complete reports are attached.

3. Physical measurements and corrosion rate calculations

The diameter measurements verified that the tubing was 2 7/8-inch tubing. The wall thickness of the tubing was measured at points where no corrosion had occurred. The following results were obtained:

0.217 inches
0.215 inches
0.216 inches
0.215 inches
Average 0.216 inches

The average wall thickness corresponded to 2 7/8-inch, 6.5 #/ft tubing, which had an initial nominal wall thickness of 0.217 inches (217 mils). Based on the total time in service of 3 years and 8 months, the calculated internal corrosion rate was 59 mpy. However, the external corrosion had to occur in the last 18 months of service. Therefore the external corrosion at the failure sites was at least 145 mpy. The corrosion rate that was due to impingement could not be accurately determined.

4. Hardness measurements

The metal hardness was measured using a Clark Rockwell Hardness gauge and the Rockwell C (RC) scale. The following measurements were obtained:

21.5 RC
21 RC
21 RC
21.5 RC
Average 21.25 RC

The average hardness corresponded to an estimated tensile strength of 107,000 psi. This value and the hardness indicated that the tubing was L-80 grade material as reported.

5. Fluid velocity calculations

Using the API-RP14E equation and the given inside diameter and flowing conditions, the fluid velocities in the tubing were calculated. Based on the production rates during these periods the following results were obtained.

Condition:	Production rates:	Fluid velocity
Flowing	64 mscf/day gas, 91 bbls/day oil, and 100 bbls/day water	0.714 ft/sec
Pumping	no gas, 50 bbls/day oil, and 340 bbls/day water	0.750 ft/sec
Gas lift	165 mscf/day gas, 20 bbls/day oil, 1000 bbls/day water	15.86 ft/sec

It was obvious that there was a substantial increase in fluid velocity when the well was converted to gas lift.

DISCUSSION OF RESULTS:

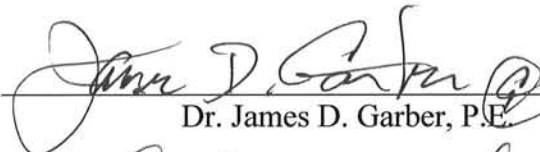
The 2 7/8-inch production tubing from the Thibodeaux #1 well has experienced severe corrosion that resulted in several failures. This well was initially flowing, then converted to pumping, and then converted to gas lift. Several sections of the tubing and two gas lift mandrels were examined. Each section had experienced some degree of corrosion. The produced fluids contained CO₂ and a small amount of H₂S. The produced water contained 44,200 mg/l of chlorides and 1,200 mg/l of acetates. The tubing had been in service a total of 3 years and 8 months.

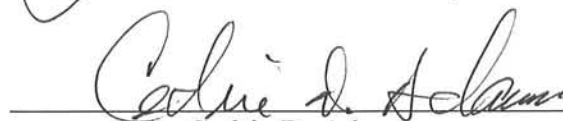
The analyses and examination identified several corrosion mechanisms that contributed to the failures. It appeared that the corrosion initiated while the well was on rod pump. Almost all of the internal corrosion was located in areas where rod wear was evident. The rod wear

removed protective scale and cold worked the tubing metal. These conditions accelerated the corrosion process. The analyses indicated that the internal corrosion was CO₂ corrosion assisted by H₂S. After the well was converted to gas lift, the flow dynamics further accelerated the CO₂/H₂S corrosion process. In addition, the flow dynamics and the presence of entrained sand in the produced fluids caused sand impingement at the leading edge of some of the pin ends. The most aggressive corrosion occurred on the external surface of the tubing. This appeared to be bacterial corrosion, which might have also attacked the internal surface of the casing.

If any of the original tubing is currently in the well, the tubing should be removed and inspected for internal and external corrosion. Any joint of tubing that has experienced cold working due to rod wear from the sucker rods should be discarded. It might be best to eliminate all of the original tubing. Since this well is now on gas lift, the problem with future rod wear will no longer exist. However, the well fluids exhibited a corrosive nature and plans should be made to introduce a corrosion inhibitor into the well to control internal CO₂ and H₂S corrosion. The problem with sand impingement has to be addressed. Eliminating the sand with sand screens or gravel packs should end this problem. If the sand cannot be eliminated, tubing collars that eliminate the gap in between the joints should be used. Either premium connectors or collars with inserts could eliminate the exposure of the leading edge of the pin. The bacteria infestation in the annulus will have to be addressed. Bactericide applications should resolve this problem. Since the external corrosion due to bacteria was so aggressive, there is the possibility of corrosion damage to the internal surface of the casing. A caliper survey should be conducted on the casing to determine the integrity of the casing. Replacing the L-80 tubing with corrosion resistant alloy (CRA), like chrome 13, should solve the internal corrosion problems, but the problem with sand impingement and bacteria will remain and will have to be addressed.

Data Analysis and Report By:


Dr. James D. Garber, P.E.


Cedric D. Adams

Garber Laboratories, Inc. is an independent consulting service. Analysis and opinions are of materials presented by our customers. Our reports are not intended for distribution to, or reliance upon by, persons other than our customers.



Figure 1
Sections of the Tubing Received for Examination



Figure 2
Gas Lift Mandrels Received for Examination



Figure 3
Section #2 from 1,800 Feet



Figure 4
Internal Surface of Section #2



Figure 5
Internal Surface of Section #2 After Cleaning



Figure 6
Internal Corrosion on Section #2



Figure 7
Section #3 from 2,900 Feet



Figure 8
Sand Impingement on Section #3



Figure 9
Section #4 from 3,300 Feet



Figure 10
Close-Up of the External Corrosion on Section #4



Figure 11
Section #6 from 5,700 Feet



Figure 12
Internal Surface of Section #6



Figure 13
Internal Surface of Section #6 After Cleaning

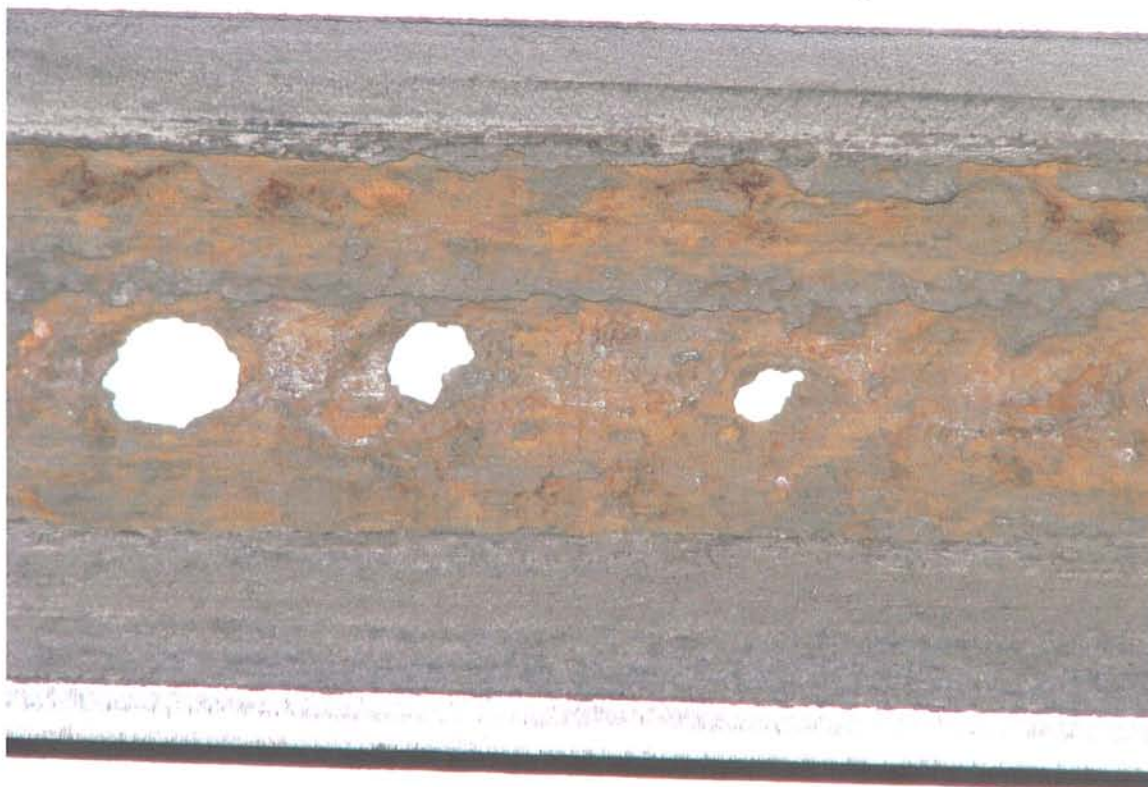


Figure 14
Internal Corrosion on Section #6



Figure 15
Section #7 from 6,800 Feet



Figure 16
Internal Surface of Section #7 After Cleaning



Figure 17
Section #9 from 8,700 Feet

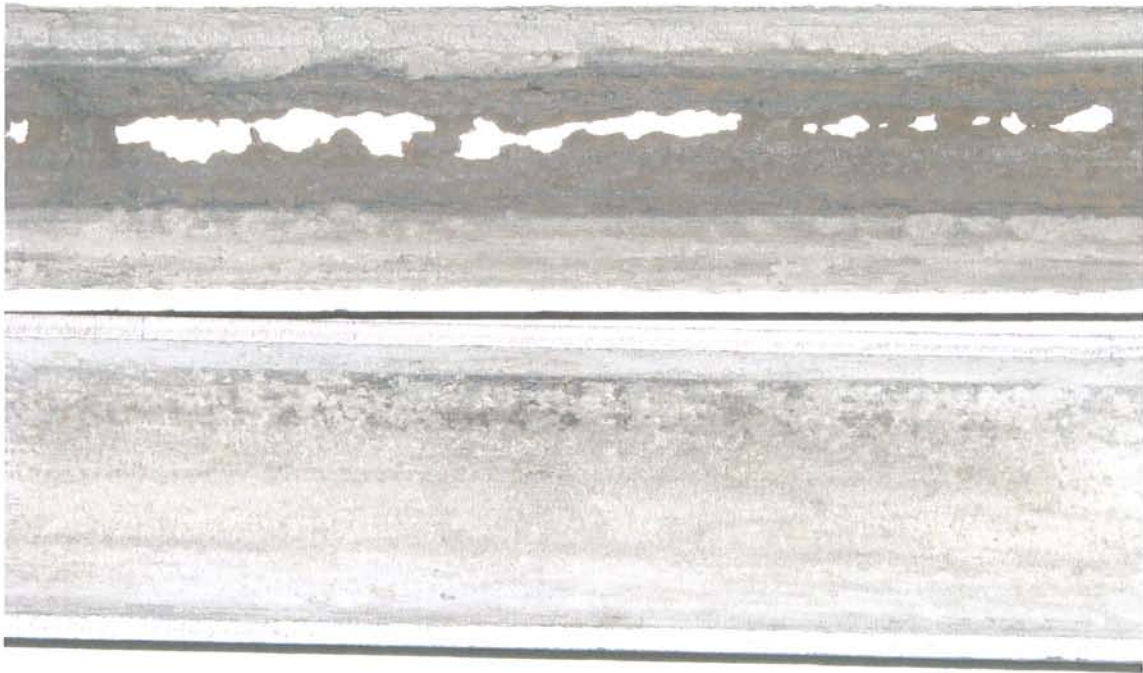


Figure 18
Internal Surface of Section #9 After Cleaning



Figure 19
External Corrosion on the Gas Lift Mandrel from 3,860 Feet



Figure 20
External Corrosion on the Mandrel



Figure 21
External Pits on the Gas Lift Mandrel from 4,100 Feet



Figure 22
External Corrosion on the Gas Lift Mandrel from 4,100 Feet



Figure 23
External Corrosion on the Gas Lift Mandrel After Cleaning

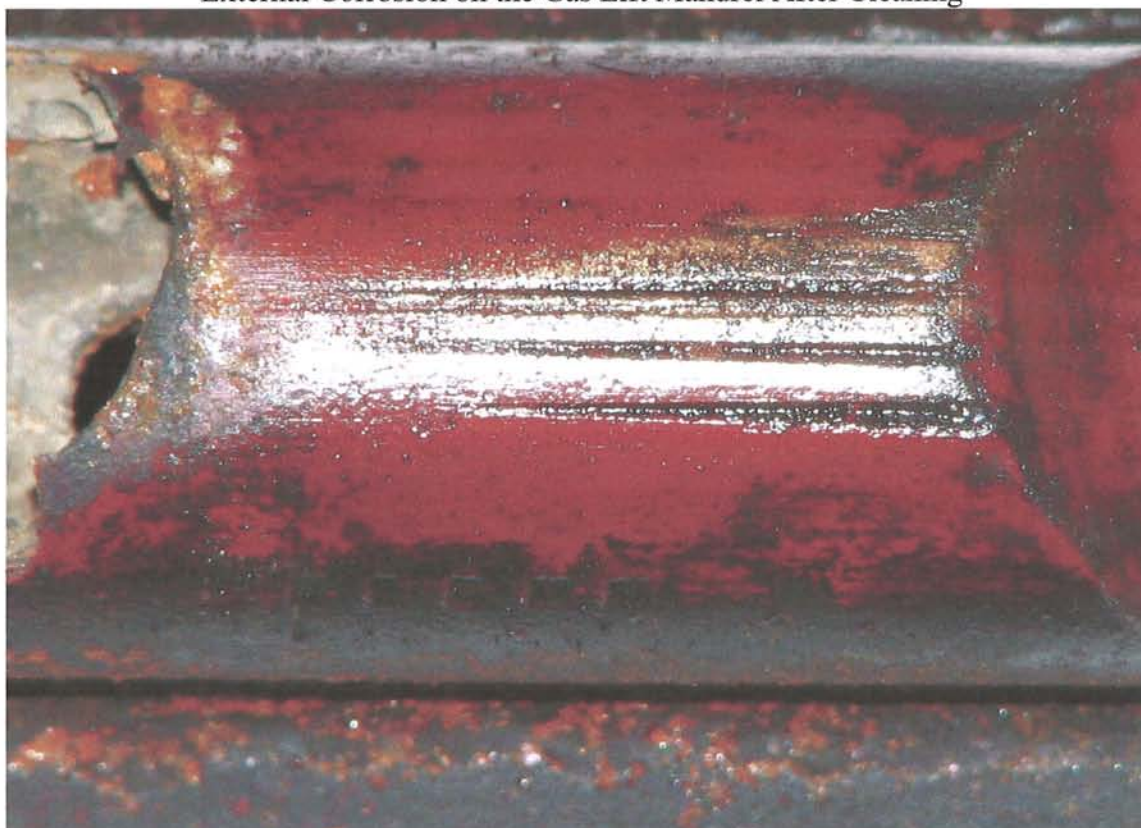


Figure 24
Mechanical Damage on the Gas Lift Mandrel from 4,100 Feet

c.d.a. and associates, inc.

Laboratory Testing, Consulting, and Corrosion Services

P.O. Box 51641 Lafayette, LA 70505 - 1472 S. College Rd, Suite 104 Lafayette, LA 70503

Office: 337-237-2342 Fax: 337-237-8982 Cedric@cda-gl.com

December 13, 2011

Mr. John Trosclair
Block T Petroleum
P.O. Box 2080
Tyler, TX 75710-2080

Re: Project Number 11-417-E, Solids Analysis by Wet Bench Methods
Location: South Bayou Malett Field, Thibodeaux Lease, Well #1
Sample: Scale from the Internal Surface of the 2 7/8-Inch Tubing at the Failure Sites

Wet Bench Analysis:

Sample Preparation: The sample was dried at 250 °F for 1 hour to remove moisture and then washed in hot xylene and dried again.

Appearance: Dark gray crystalline solids
Moisture Content: 2.2 % by weight
Xylene Soluble Content: 3.8 % by weight

The clean dried sample was dark gray crystalline material. A portion of the dried sample was placed in the muffle furnace at 950 °F for 30 minutes. The ash was gray crystalline material.


Loss on Ignition: 9.7 % by weight

Composition of the Dried Solids After the Xylene Wash:

Magnetite (Fe ₃ O ₄)	-	36 %	Major
Acid insoluble material	-	19 %	Minor
Siderite (FeCO ₃)	-	18 %	Minor
Iron Sulfide (FeS)	-	11 %	Minor
Calcite (CaCO ₃)	-	12 %	Minor
Hematite (Fe ₂ O ₃)	-	4 %	Trace

Note: The gray acid insoluble material had a crystalline structure and appeared to be sand. The sample was negative for NORM.

Analyst:


Cedric D. Adams

c.d.a. and associates, inc.

Laboratory Testing, Consulting, and Corrosion Services

P.O. Box 51641 Lafayette, LA 70505 - 1472 S. College Rd, Suite 104 Lafayette, LA 70503

Office: 337-237-2342 Fax: 337-237-8982 Cedric@cda-gl.com

December 13, 2011

Mr. John Trosclair
Block T Petroleum
P.O. Box 2080
Tyler, TX 75710-2080

Re: Project Number 11-417-E, Solids Analysis by Wet Bench Methods
Location: South Bayou Malett Field, Thibodeaux Lease, Well #1
Sample: Scale from the External Surface of the 2 7/8-Inch Gas Lift Mandrels at the Failures

Wet Bench Analysis:

Sample Preparation: The sample was dried at 250 °F for 1 hour to remove moisture and then washed in hot xylene and dried again.

Appearance: Light gray crystalline solids
Moisture Content: 1.1 % by weight
Xylene Soluble Content: 10.5 % by weight

The clean dried sample was light gray crystalline material. A portion of the dried sample was placed in the muffle furnace at 950 °F for 30 minutes. The ash was gray crystalline material.

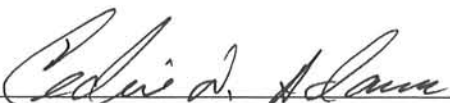
Loss on Ignition: 22.7 % by weight

Composition of the Dried Solids After the Xylene Wash:

Acid insoluble material	-	57 %	Major
Iron Sulfide (FeS)	-	20 %	Minor
Siderite (FeCO ₃)	-	12 %	Minor
Magnetite (Fe ₃ O ₄)	-	6 %	Minor
Hematite (Fe ₂ O ₃)	-	5 %	Trace
Calcite (CaCO ₃)	-		Negative

Note: The gray acid insoluble material had a crystalline structure and appeared to be sand. The sample was negative for NORM.

Analyst:


Cedric D. Adams

c.d.a. & associates, inc.

API RP-14E Calculation for Erosion Corrosion Velocity	
Reference:	Block T Petroleum
Location:	Thibodeaux #1, gas lift
Pressure in psig	50
Temperature in Deg. F	115
Gas Rate in MMSCF	0.165
Oil Rate in BBLS	20
Water Rate in BBLS	1000
Mol. Wt. of Gas (16)	16
SpGr of Gas (.65)	0.65
SpGr of Oil (.875 for API 30)	0.825
SpGr of Water (1.0)	1.055
Pipe ID in Inches	2.441
Results:	
Mean Density	8.14
Erosional Velocity in ft/sec	35.0503791
Erosional Velocity w/sand in ft/sec	21.0302275
Actual Velocity in ft/sec	15.8647636

API RP-14E

c.d.a. & associates, inc.

API RP-14E Calculation for Erosion Corrosion Velocity		
Reference:	Block T Petroleum	
Location:	Thibodeaux #1, pumping	
Pressure in psig	50	
Temperature in Deg. F	120	
Gas Rate in MMSCF	0.0001	
Oil Rate in BBLS	50	
Water Rate in BBLS	340	
Mol. Wt. of Gas (16)	16	
SpGr of Gas (.65)	0.65	
SpGr of Oil (.875 for API 30)	0.825	
SpGr of Water (1.0)	1.055	
Pipe ID in Inches	2.441	
Results:		
Mean Density	63.31	
Erosional Velocity in ft/sec	12.5675284	
Erosional Velocity w/sand in ft/sec	7.54051701	
Actual Velocity in ft/sec	0.75030861	

API RP-14E

c.d.a. & associates, inc.

API RP-14E Calculation for Erosion Corrosion Velocity		
Reference:	Block T Petroleum	
Location:	Thibodeaux #1, flowing	
Pressure in psig	1020	
Temperature in Deg. F	120	
Gas Rate in MMSCF	0.064	
Oil Rate in BBLS	91	
Water Rate in BBLS	100	
Mol. Wt. of Gas (16)	16	
SpGr of Gas (.65)	0.65	
SpGr of Oil (.875 for API 30)	0.825	
SpGr of Water (1.0)	1.055	
Pipe ID in Inches	2.441	
Results:		
Mean Density	31.87	
Erosional Velocity in ft/sec	17.7128815	
Erosional Velocity w/sand in ft/sec	10.6277289	
Actual Velocity in ft/sec	0.71460431	

API RP-14E



Coastal Chemical Co., L.L.C.
 6133 Hwy 90 East; Lafayette, La 70518
 PHONE: 800.333.1522 FAX 337.330.8092

WATER ANALYSIS REPORT

Company: **Block T Petroleum**
 Field or Plant: **South Bayou Mallet**
 Lease/Well #:
 Sample Point: **Thibodeaux #1**
 Date Submitted: **6/6/2011**

Sample Number: **11060195-03**
 Date Sampled: **6/4/2011**
 Sampled By: **John Knickerbocker**
 Customer Contact
 Account Rep: **Team Sales**

BWPD:	MMCF:	BOPD:	Iron Loss/(lb/Day):
--------------	--------------	--------------	----------------------------

<u>CATIONS</u>	<u>mg/L</u>	<u>mEq/L</u>	<u>ANIONS</u>	<u>mg/L</u>	<u>mEq/L</u>
Strontium	160	3.8	Acetate	1200	
Sodium(calc)	25772.6	1120.5	Formate	< 5	
Manganese	1.9		Sulfate	23.4	0.5
Magnesium	380	30.9	Chloride	44200	1245.1
Iron	12	0.4	Bicarbonate	537	8.8
Calcium	2000	98.5			
Barium	15	0.2			

Total Dissolved Solids (mg/L)	74302
--------------------------------------	-------

<u>DISSOLVED GASES:</u>			
<u>Oxygen ppb</u>	<u>Oxygen ppm</u>	<u>Hydrogen Sulfide</u>	<u>Carbon Dioxide ppm</u>
N/A	<.05	<u>ppm</u> <.1	32

<u>PHYSICAL PROPERTIES:</u>			
<u>pH</u>	<u>Field Temperature °F</u>	<u>Specific Gravity</u>	<u>Alkalinity (as CaCO3)</u>
7.2	118	1.055	440.34

<u>Scaling Index</u>		
<u>Calcium Carbonate</u>	<u>Temperature (deg F)</u>	<u>Calcium Sulfate</u>
0.66	100°	-2174.6
0.77	110°	-2150.6
0.99	120°	-2134.6

Interpretation: Positive scaling tendency if >0, negative if < or =0.

Date Analyzed:
6/6/2011

Analyst:
cromero

The data presented in this document are typical only and not specifications. The information and suggested uses are based on evaluations believed reliable. No guarantee or warranties are expressed or implied, however, including the implied warranty of merchantability and fitness for particular purpose. Coastal Chemical Co., LLC disclaims any liability in the use of these data, including possible infringement of patent.